

Research Paper

Cite this article: Schieler S, Schneider C, Andrich C, Döbereiner M, Luo J, Schwind A, Thomä RS, Del Galdo G (2020). OFDM waveform for distributed radar sensing in automotive scenarios. *International Journal of Microwave and Wireless Technologies* **12**, 716–722. <https://doi.org/10.1017/S1759078720000859>

Received: 18 November 2019
Revised: 29 May 2020
Accepted: 29 May 2020
First published online: 1 July 2020









Keywords:

Microwave measurements; radar signal processing and system modeling; radar architecture and systems

Author for correspondence:

Steffen Schieler,
E-mail: steffen.schieler@tu-ilmenau.de

OFDM waveform for distributed radar sensing in automotive scenarios

Steffen Schieler¹ , Christian Schneider^{1,2} , Carsten Andrich¹ ,
Michael Döbereiner² , Jian Luo³ , Andreas Schwind¹ , Reiner S. Thomä¹ 
and Giovanni Del Galdo^{1,2} 

¹Technische Universität Ilmenau, Ilmenau, Germany; ²Fraunhofer Institute for Integrated Circuits, Ilmenau, Germany and ³Huawei Technologies Düsseldorf GmbH, Munich, Germany

Abstract

In this paper, an orthogonal frequency-division multiplexing (OFDM) waveform radar sensing approach is demonstrated based on field measurements at C-band. We demonstrate a concept that is based on the exploitation of typical wireless communication transmissions to perform passive, distributed radar sensing. Our concept is based on an OFDM radar that operates in the modulation symbol domain and can be well integrated into existing OFDM receivers. The measurement setup and the signal processing steps for the OFDM radar are described. The results show that the passive, distributed radar sensing approach can be used to detect and localize moving cars and even pedestrians in automotive intersection scenarios.

Introduction

Along with the rapid deployment and evolution of mobile communication throughout the last 20 years, orthogonal frequency-division multiplexing (OFDM) has developed to be a common waveform in many such systems. The limited spectral resources required to enable wireless communication are valuable for any mobile network operator. However, those limitations also have increasing importance in the field of radar sensing.

Primarily due to the development in the area of autonomous driving, more and more new cars are equipped with radar sensors to enable intelligent transport systems. Often, those radar sensors are based on the frequency-modulated continuous-wave (FMCW) waveform and operate from an ego perspective, meaning each car uses them to obtain awareness on the current traffic situation. However, the increasing number of deployed radar units inevitably leads to multiple-access problems. Interference from the different radar sensors can cause ghost targets, increased false-alarm rates, and reduced receiver sensitivity [1]. One approach to combat those problems is to add communication abilities to the radar, e.g. as in [2]. The authors propose to add an OFDM-based communication system to a FMCW-based radar by using frequency-division multiplexing. While this approach reduces the interference, it also creates additional overhead for the radar system and occupies auxiliary spectral resources. Another proposal, called cooperative passive coherent location (CPCL) and presented in [3], aims at the re-use of OFDM wireless communication resources for radar sensing. Instead of operating from an ego perspective, the sensing is performed in a bi-static geometry (known from passive radar) with distributed sensors and based on mobile communication transmissions. Such an OFDM radar enables simultaneous communication and radar sensing on the same resources without the requirement of an extra waveform. Furthermore, not following the typical correlation-based passive radar approach, utilizing OFDM allows for a more intuitive, modulation symbol-based radar processing. This approach, termed OFDM radar and first presented by [4], shares many signal processing steps with the communication system, and hence provides an efficient opportunity for simultaneous communication and distributed radar sensing.

The radar sensing abilities of an OFDM radar for a monostatic setup are described and demonstrated in [4]. In contrast, this paper¹ presents an experimental demonstration of the OFDM radar technique for a distributed radar sensing system with bi-static geometry in an automotive scenario. With the evaluation, we attempt to demonstrate its general feasibility and efficiency for an approach as introduced in [3]. We start by providing a short introduction to the OFDM radar in section “OFDM radar sensing”. Then a brief description of the measurement setup and the signal processing steps are given in section “Setup and signal processing”. The results presented in section “Results” demonstrate the visibility of the radar targets. Furthermore, we provide the raw target positioning results of the measurements obtained from

¹Parts of this paper were presented and published at the 16th EuRAD conference, 2019.

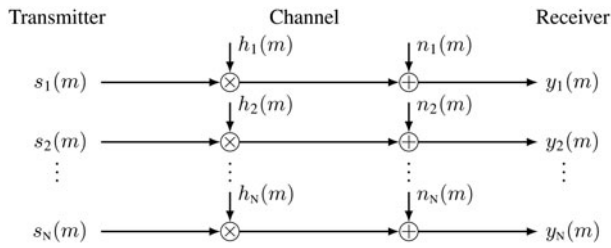


Fig. 1. Simplified relationship between transmitted and received modulation symbols in OFDM.

the simple discrete Fourier transform (DFT) approach based on spatial ellipse intersection. Finally, section “Conclusion and outlook” presents the conclusion and future research topics.

OFDM radar sensing

A detailed description of the OFDM radar principle from the radar domain is given in [4]. For this paper, we are approaching the description from the communication perspective. We start by looking at a single channel estimate obtained from an OFDM symbol in complex baseband. In a second step, it is extended to span multiple OFDM symbols and then shown how the delay-Doppler response $|h(\tau, f_b)|^2$ is obtained.

According to [5], the relationship between the transmitted symbols $s_i(m)$ and received symbols $y_i(m)$ of a m -th OFDM symbol with N subcarriers can be written as

$$y(m) = \text{diag}(h(m)) \cdot s(m) + n(m) \tag{1}$$

where $n(m)$ denotes additive noise. This relationship is also illustrated in Fig. 1. In the typical communication case, the receiver (Rx) knows the modulation contents of some subcarriers in the received OFDM symbol, called reference symbol (RS). It can then use those RS to estimate the channel and equalize $y(m)$ to obtain an estimate of the originally transmitted modulation symbols. Assuming that the receiver can recover an error-free copy of the transmitted symbol (e.g. due to additional methods such as error correction), it can re-estimate the channel gain on each i th subcarrier by applying an inverse filter operation.

$$\tilde{h}_i(m) = \frac{y_i(m)}{s_i(m)} \tag{2}$$

Now assume a stream of M OFDM symbols, such that $m = 1, 2, \dots, M$. As the receiver repeats the channel estimation for each OFDM symbol m , we obtain the matrix in (3).

$$\tilde{H} = [\tilde{h}(1) \quad \tilde{h}(2) \quad \dots \quad \tilde{h}(M)]_{N \times M} \tag{3}$$

We see that one interpretation of \tilde{H} is as a sampled two-dimensional representation of the channel in frequency f and time t . Therefore, \tilde{H} can be interpreted as a complex baseband representation of the time-variant channel transfer function $H(f, t)$. According to [6], the channel representation can be transformed into a representation in $h(\tau, f_b)$ using a two-dimensional Fourier transform. To obtain the representation of the channel in the delay-Doppler domain (matrix D) a two-dimensional DFT is applied. For simplicity, the elements of the

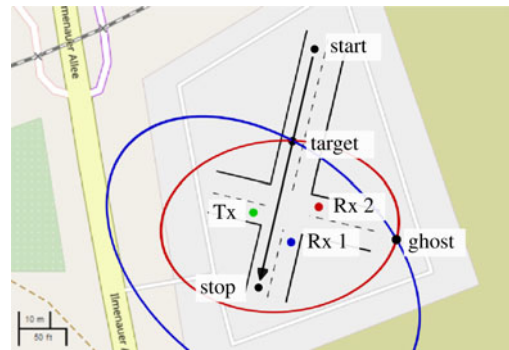


Fig. 2. Measurement area in Ilmenau with an illustration of the setup and track. The intersection of two ellipses from the Rx’s provides the actual target and a ghost-target positions. The map material is taken from [7].

matrices D and \tilde{H} are now denoted by $d_{k,l}$ and $h_{n,m}$, respectively.

$$d_{k,l} = \sum_{n,m=1}^{N,M} \tilde{h}_{n,m} \exp\left(j2\pi k \frac{n-1}{N} - j2\pi l \frac{m-1}{M}\right) \tag{4}$$

The achieved processing gain G (according to [4]) depends on the dimensions of the matrix D .

$$G = N \cdot M \tag{5}$$

In the derivation we have assumed that the receiver can estimate the complex channel gain on every subcarrier. However, it is also possible to obtain the radar estimate using just the *a priori* known RS, for example, by zeroing the channel gains on the unknown subcarriers. Therefore, radar localization based on the public RS, e.g. in case of 5G, the channel state information reference signal (CSI-RS), is possible but likely experiences reduced performance compared to utilizing all the available resources. The question of useful resources quickly transforms into one for specific radar resource allocation schemes, for which the discussion is beyond the scope of this paper. For now, we will, therefore, stick to the assumption of full knowledge on the modulation symbols in the transmitted signal.

The processing scheme explained above potentially yields the same results as the two-dimensional ambiguity function usually used in passive radar sensing, meaning that target detection can be performed using either. However, the DFT-based method has several benefits, namely a lower sidelobe level and a significantly reduced computational complexity (see [4]). Nevertheless, to successfully apply the processing scheme, the radar receivers have to be synchronized with the stream of transmitted OFDM symbols, as otherwise the system model in (1) and the inverse filter (2) are invalid. As synchronization is mandatory for any communication system (and therefore based on public *a priori* knowledge about the system), OFDM radar sensors can exploit the build-in mechanisms to perform their self-synchronization and subsequently benefit from the lower complexity of the processing scheme.

Setup and signal processing

The measurements were performed on an empty parking lot in Ilmenau, Germany. For the measurement, it was blocked for public traffic. However, a suburban road with low traffic density and a train track are also within the perimeter (see Fig. 2). Table 1 shows

Table 1. Measurement setup and signal parameters

Name	Value
Carrier frequency	5.2 GHz
Transmit power	33 dBm
Antennas	5 dBi, omnidirectional (azimuth)
Bandwidth (used)	100 MHz (80 MHz)
Subcarriers (used)	6400 (5120)
Subcarrier spacing	15.625 kHz
Symbol length	64 μ s
Modulation	Phase-only, crest factor optimized

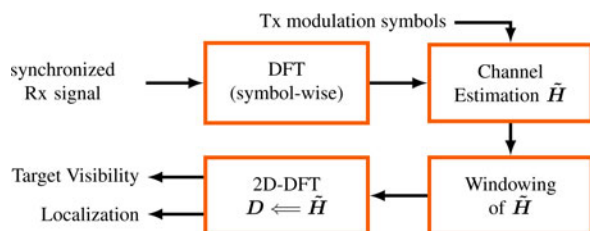
the parameters for our OFDM measurement signal, as continuously transmitted by the transmitter (Tx). The measurement equipment was built into passenger cars, and the signal was transmitted/received via magnet-mounted antennas on the roofs. All used antennas provide a roughly omnidirectional characteristic in the azimuth plane and a gain of 5 dBi.

After starting the measurement, the radar target accelerates, passes between the intersection between Tx and Rx, and breaks shortly after passing Rx 1 (see Fig. 2).

Evaluation of the measurement is performed offline with the recorded complex baseband data; the applied steps are outlined in Fig. 3. As explained in section “OFDM radar sensing”, we assume the originally transmitted modulation symbols are available to the receivers. First, each received stream is synchronized in the time domain by using a cross-correlation approach to detect the start of the first OFDM symbol. Therefore, in the following evaluation, the strongest channel component (typically the line-of-sight (LOS), is roughly shifted toward the $\tau = 0$ ns delay bin. This shift does not distort the overall results, as only the relative time difference between the LOS and the target component is of interest.

Target visibility

One crucial factor in the evaluation is the achievable resolution with an OFDM radar. As for this evaluation, we rely on the DFT processing, it is accordingly defined by the dimensions and element spacing of the matrix D . We processed only the used subcarriers ($N = 5120$), which correspond to a delay resolution of $\Delta\tau = 12.5$ ns. The Doppler resolution Δf_D is defined by the inverse of the observation time window length T_w that is spanned by the M successive OFDM symbols. To ensure a sufficient signal-to-noise ratio gain, and Doppler resolution, we set

**Fig. 3.** Signal processing steps for the evaluation.

$T_w = 128$ ms which corresponds to 2000 successive OFDM symbols and $\Delta f_D = 7.8125$ Hz. For this configuration, the expected processing gain from the DFT processing according to (5) is $G = 70.1$ dB. The relative noise level in the normalized results was estimated at -80 dB, and therefore the results are thresholded accordingly. To validate the results, positions of the Tx, Rx, and target were recorded in the measurement and used to provide a ground truth.

Random cars or pedestrians (for which no ground truth is available) passed by the measurement area as well, creating a more realistic environment.

Localization performance

After studying the visibility of the different radar targets in the delay-Doppler domain, the next step was to localize the automotive radar target. A simple peak-search algorithm from image processing was used to extract the targets delay and Doppler properties from each of the processed windows. The LOS was identified in each window by assuming that it always corresponds to the strongest detected peak in the channel. The remaining detected peaks were treated as possible target paths, from which the respective time difference of arrival (TDoA) measurement (relative to the LOS delay) and Doppler-shift properties were extracted.

By combining TDoA measurements with the known distance between Tx and respective Rx, ellipses of constant bi-static range with the Tx and corresponding Rx in the foci points can be obtained (see Fig. 2). The target can be located on any of the points belonging to an ellipse.

Due to hardware limitations and initial measurement purposes, our setup consisted of only two receivers, from which only two ellipses for a single target can be extracted in each processing window. However, to perform an unambiguous localization based on spatial ellipse intersection in a plane, at least three ellipses are required. Due to this, the intersection of the two obtained ellipses also reveals the positions of a ghost target, as illustrated by Fig. 2. We note that by applying *a priori* knowledge of the intersection scenario, the ghost target could also be removed with a tracking filter as its overall trajectory is unmeaningful.

Results

During the measurement, the Rx and Tx are stationary. The Doppler shift caused by a moving target will be non-zero, while solely paths reflected by static objects contribute no Doppler shift. First, we present the visibility of different radar target types, then we study the raw localization of the OFDM radar approach based only on the DFT processing.

Target visibility

As a first step after performing the measurements, we wanted to study the target visibility as described by section “Setup and signal processing”. The measurement site was located close to a public road where cars and pedestrians passed the site randomly. Therefore, we are going to present two different types of visibility results. First, we analyze the visibility of the actual car radar target and then those of random targets.

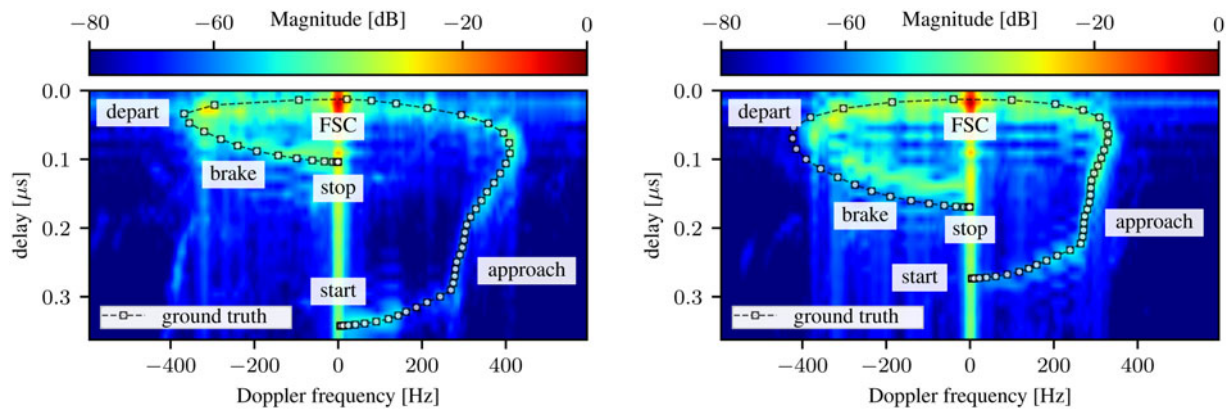


Fig. 4. Max-hold results of Rx 1 (left) and Rx 2 (right). The car target is successfully detected and matches the expectations from the ground truth.

Car target

As depicted in Fig. 2, the target car passes between the Tx and Rx during the measurement. Doppler- and delay-wise, the process can be divided into four stages. First, the approaching stage, in which the target moves toward the intersection. In this stage, the Doppler shift is positive, as the observed frequency increases due to the compression of the waves. The delay decreases in this stage. Second, the forward scattering stage (FSC), when the target is located between the Tx and respective Rx. Here, the Doppler shift is zero and the delay corresponds to that of the LOS. Third, the departing stage, in which the target is moving away from the Tx and Rx. Now the Doppler shift is negative, as the wavelength is now increasing due to the motion of the target. The delay is now increasing again, as does the distance for the reflected target path. Last, the braking stage, in which the target is braking and the Doppler shift decreases down to 0 Hz, while the delay increases. With a peak target velocity of 16 m/s, the maximum expected bi-static Doppler shift according to [8, chapter 3] is 555 Hz.

A max-hold algorithm was used to construct a single plot from all normalized windows processed during the measurement in Fig. 4, while Fig. 5 shows single-window snapshots from both Rx's during the approaching stage. The additional sidelobes in Fig. 4, especially visible during the departing and braking stage, are artifacts captured due to the max-hold algorithm.

We observe that the radar target reflections are visible and match the ground truth considering the resolution limits from the applied signal processing. Deviations, e.g. during the braking stage in Rx 2, are assumed to result from variations in the resolution of the recorded ground truth positions and the extended target dimensions. The limit for the maximum Doppler shift is maintained.

Due to the smaller additional distance of the reflected signal from Tx-Rx 2 (compared to Tx-Rx 1), the target delay is smaller at Rx 2. Furthermore, we can see that the target is roughly 50 dB below the LOS component regarding received power at the snapshot in both Rx's.

Pedestrian target

The measurement site is located close to a public road with a sidewalk (see Fig. 2). Therefore, the measurements also contain reflections from those road users, whose presence has been validated in post-processing using a video of the measurement scene. As the actual radar target was a car, we now focus on the pedestrian

targets of opportunity captured during the measurement. Due to their naturally lower velocity, pedestrians do cause a smaller Doppler shift compared to the cars. Assuming a typical velocity of 1 m/s, the maximum expected Doppler shift for the given carrier frequency is around 34 Hz and therefore resolvable with the Doppler resolution of $\Delta f_D = 7.8125$ Hz.

One especially illustrative situation was found when a pedestrian and a car passed by on the nearby, public road (see Fig. 2) simultaneously. Both can be detected in the corresponding delay-Doppler plot in Fig. 6(a). Thus, demonstrating the suitability of the proposed localization scheme, as both the pedestrian and the target can be separated in the results by their Doppler shifts even though they cause similar delays.

The situation in Fig. 6(b) provides further proof of the separability. When measurement personnel was walking away from the Rx 1 after starting the measurements, the corresponding delay-Doppler plots clearly show a distinct peak, even though the delay is close to the LOS, and the peaks differ by about 30 dB.

Radar localization

After confirming the visibility of the targets in the measurement data, the next step is to extract the target parameters and perform the localization. The respective path parameters were extracted using a two-dimensional peak search from image processing with a 3 dB offset toward the -80 dB noise threshold. Due to the noise and signal processing, the $|h(\tau, f_D)|^2$ also contains peaks from clutter, sidelobes and hardware imperfections. For each such peak, an ellipse can be obtained, which would give rise to a large number of ghost targets if no additional measures are taken. An efficient way to counter those ghost targets is the use of tracking techniques, e.g. as described in [9]. However, tracking techniques are beyond the scope of this paper and instead a simple parameter filter based on the ground truth was applied. The ground truth filter uses the known locations of the Tx, Rx's and the target to predict the targets delay- and Doppler properties for each window and remove any paths whose parameters are not sufficiently close to the ground truth parameters. As a result, most of the clutter is removed and a much cleaner result is obtained. We note that such a filter can only be used for research purposes and is not suited for real system implementation.

Even though both, delay- and Doppler properties, are estimated by the peak-search, we use only the delay to obtain the

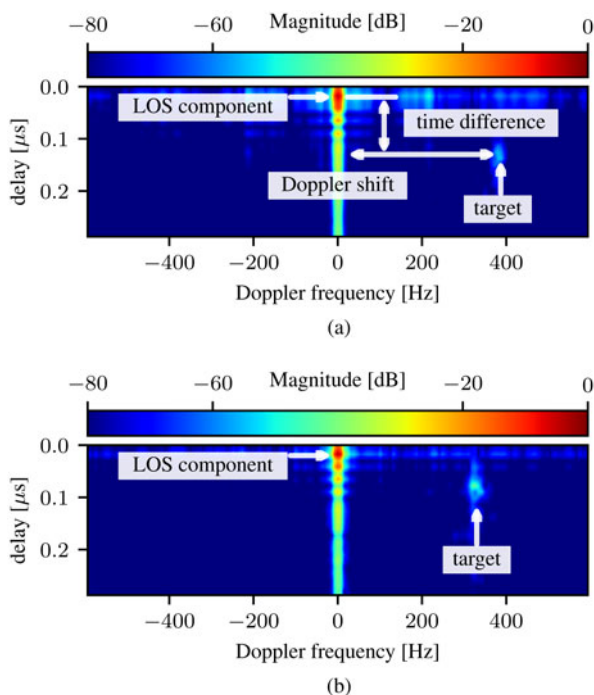


Fig. 5. Associated $|h(\tau, f_d)|^2$ snapshots during the approaching stage. (a) Rx 1. (b) Rx 2.

spatial ellipses. The parameters obtained after the peak-search and subsequent ground truth filtering are presented in Fig. 7. While the ground truth and estimates are a close match, a step-wise progression and adaption of the parameters due to the Fourier-resolution limit can be observed. Furthermore, it can be seen that the peak-search fails in some situations, especially in the FSC, where no peaks are detected. As good estimates are obtained mainly in the approaching stage, we decided to limit the localization evaluation only to this stage. We note, however, that it is possible to obtain more smooth and continuous TDoA estimates by using high-resolution parameter estimation (HRPE), e.g. as introduced by [10, 11], during all stages of the measurement. DFT-based interpolation is not guaranteed to improve the results due to additional closeby paths, e.g. from the ground reflection.

In order to get the ellipses, the TDoA measurements from each receiver are combined with *a priori*-knowledge about the LOS propagation delay. For each processed window during the

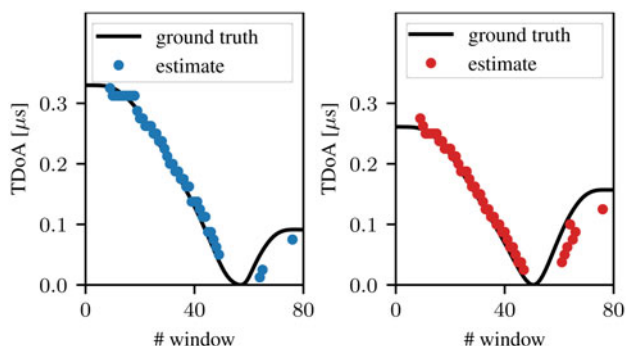


Fig. 7. Target TDoA estimates after ground truth filtering at Rx 1 (left) and Rx 2 (right).

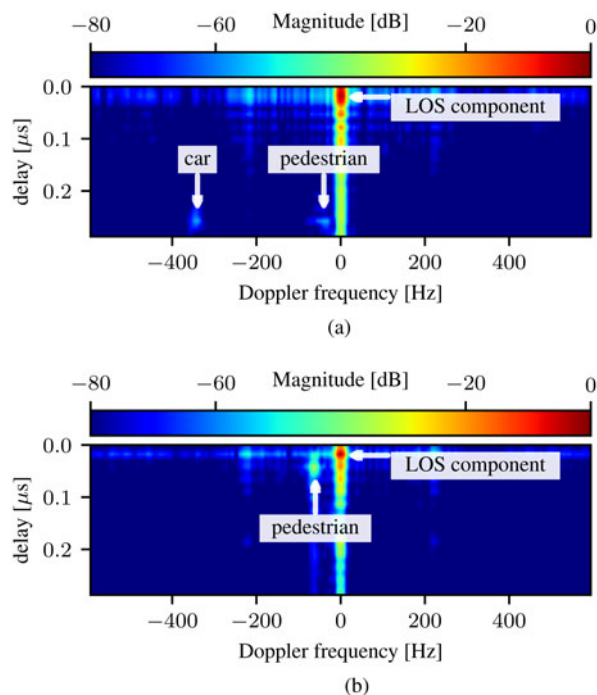


Fig. 6. Doppler separability of moving pedestrian and car targets. (a) Separability of pedestrian and car with similar delay. (b) Separability of a pedestrian close to strong LOS.

approaching stage, ellipses are constructed from the estimated parameters at each receiver. After calculating the intersection of both ellipses, the found positions are plotted in Fig. 8 together with the target and ghost-target trajectories. The obtained results show that the estimated positions and trajectory are fairly close to the ground truth at closer range, as the localization error seems to decrease while the target approaches the intersection. As explained earlier, ghost-target estimates (as marked in Fig. 8) are expected from the lack of a third receiver. Due to the limited range resolution of 3.75 m, we observe that the DFT processing results in discrete target positions.

As the TDoA estimates contain a maximum error of $\pm \Delta\tau$, the ellipses form a corresponding tube around the true value. Depending on the condition of both ellipses toward each other, the area enclosed by the tube intersection becomes either larger or smaller. One way to account for this factor is to use the geometric dilution of precision (GDOP), which describes how an error in the measurement affects the localization result. To obtain the GDOP, we use the approximation method put forward in [8, chapter 6] under the assumption of uncorrelated errors at both Rxs and combined the values for cross- and downrange by taking the root of the sum of squares. The results illustrated in Fig. 9 reveal the ellipse intersections are particularly ill-conditioned during the targets approaching phase with values ranging from 8 to 10 dB. The additional factor from the GDOP linearly increases the systematic Fourier-resolution error and explains the deviation between the estimated positions and ground truth. This is also backed-up by the ghost position estimates which agree better with their respective ground truth, as they exhibit lower GDOP. Additionally, the error was verified by repeating the positioning using the ground truth values shown in Fig. 7 filtered to Fourier resolution. The

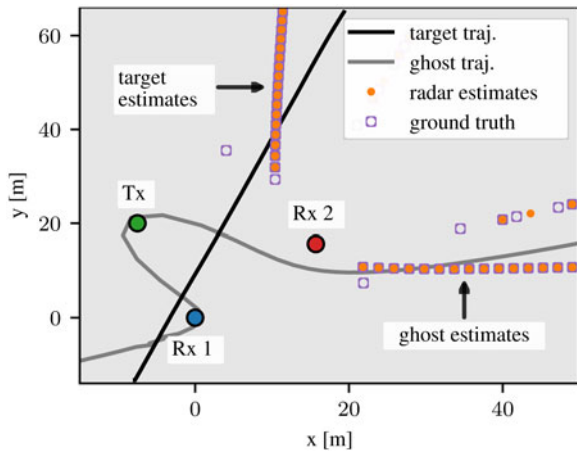


Fig. 8. Estimated target (and ghost) positions with the two-dimensional DFT approach. Estimates suffer from the insufficient resolution and poor GDOP, which was verified by performing the localization with TDoA ground truth values of equal resolution (purple circles).

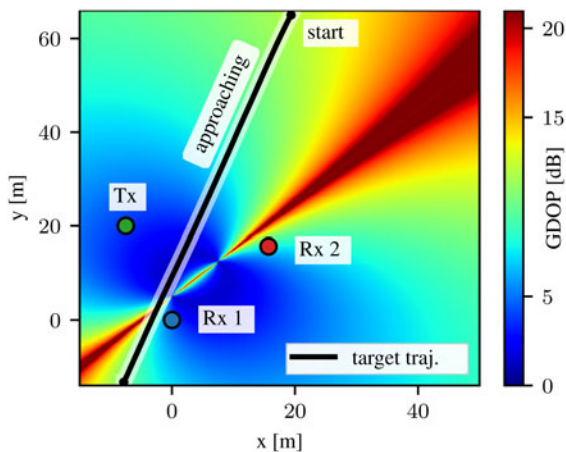


Fig. 9. The GDOP for the measurement scenario describes how errors in the measurement affect the localization result. During the approaching stage, it scales the systematic error from the limited resolution.

obtained position estimates (purple circles) align very well with the DFT results. While this explains the positioning error, it also proves the two-dimensional DFT approach alone is not sufficient to achieve satisfactory localization results in the scenario.

Conclusion and outlook

This paper builds on the concept of CPCL, an OFDM-based, distributed radar sensing approach, that applies to mobile communication scenarios [3]. Due to the nature of a communication system, the placement of the Tx/Rx corresponds to that of passive radar. A description of the OFDM radar from the mobile communication perspective shows that many signal processing steps are similar to those in communication systems.

With the evaluation of the field measurement, we demonstrate the general feasibility of the approach for distributed radar sensing in automotive applications. The results reveal that it is

possible to detect cars and even pedestrians in the bi-static setup using the OFDM-based communication signals and signal processing. The localization results further reveal that it is possible to perform target localization with the approach, even though the results are degraded due to the limited resolution of the signal processing and geometric conditions in the measurement scenario. However, the estimated positions achieve good accuracy under the given constraints and serve as further proof that distributed, passive radar sensing based on OFDM waveform is not only possible but also reasonable.

Future study items must evaluate the usage of more advanced signal processing techniques, such as HRPE and tracking, to improve localization performance. To demonstrate the proposed scheme with the constraints of realistic mobile communication systems, the influence of multiple-access resource allocation schemes is also of interest.

Acknowledgements. The research has been funded by the Federal State of Thuringia, Germany, and the European Social Fund (ESF) under the grant 2018 FGR 0082.

References

1. Bourdoux A, Parashar K and Bauduin M (2017) Phenomenology of mutual interference of FMCW and PMCW automotive radars. *2017 IEEE Radar Conference (RadarConf)*.
2. Aydogdu C, Garcia N, Hammarstrand L, Wymeersch H (2019) Radar communications for combating mutual interference of FMCW radars. *2019 IEEE Radar Conference (RadarConf)*.
3. Thomä RS, Andrich C, Galdo GD, Döbereiner M, Hein MA, Käske M, Schäfer G, Schieler S, Schneider C, Schwind A and Wendland P (2019) Cooperative passive coherent location: a promising 5G service to support road safety. *IEEE Communications Magazine* 57(9), 86–92.
4. Sturm C and Wiesbeck W (2011) Waveform design and signal processing aspects for fusion of wireless communications and radar sensing. *Proceedings of the IEEE* 99(7), 1236–1259.
5. Debbah M (2004) Short Introduction to OFDM. White Paper, Mobile Communications Group, Institut Eurecom.
6. Bello P (1963) Characterization of randomly time-variant linear channels. *IEEE Transactions on Communications* 11(4), 360–393.
7. OpenStreetMap contributors (2020) Map retrieved from <https://www.openstreetmap.de>, <https://www.openstreetmap.org>.
8. Willis NJ (2007) *Advances in bistatic radar*. Raleigh, NC (USA): SciTech Publishing Inc.
9. Daun M (2007) Multistatic target tracking for non-cooperative illuminating by DAB/DVB-T. *OCEANS 2007 - Europe*.
10. Döbereiner M, Käske M, Schwind A, Andrich C, Hein MA, Thomä RS and Galdo GD (2019) Joint high-resolution delay-doppler estimation for bi-static radar measurements. *16th European Radar Conference (EuRAD)*.
11. Thomä RS, Landmann M, Sommerkorn G and Richter A (2004) Multidimensional high-resolution channel sounding in mobile radio. *Proceedings of the 21st IEEE Instrumentation and Measurement Technology Conference*.



Steffen Schieler received the B.Sc. and M.Sc. degrees in electrical engineering and information technology from Technische Universität Ilmenau, Germany, in 2016 and 2018, respectively. He is currently a researcher with the Electronic Measurement and Signal Processing Group at the same university, and Ph.D. student with a focus on signal processing and machine learning for radar applications.



Christian Schneider received his Diploma degree in electrical engineering from the Technische Universität Ilmenau, Germany in 2001. His research interests are multi-dimensional channel sounding, characterization, and modeling for single and multi-link cases in cellular and vehicular networks at micro and millimeter wave bands. He is also active in adaptive space-time signal processing and passive coherent

location. He received the best paper awards at the European Wireless conference in 2013 and European Conference on Antennas and Propagation in 2017. He has authored more than 130 publications. He is currently pursuing the Dr.-Ing. degree with the Institute for Information Technology at the Technische Universität Ilmenau.



Carsten Andrich received the B.Sc. and M.Sc. degrees in electrical engineering and information technology from Technische Universität Ilmenau, Germany, in 2014 and 2016, respectively. He is a researcher with the Electronic Measurement and Signal Processing Group at the same university and pursuing the Dr.-Ing. degree. His research interests include high-precision measurement applications for

software-defined radio devices and efficient signal processing algorithms.



Michael Döbereiner received the B.Sc. and M.Sc. degrees in electrical engineering and information technology from Technische Universität Ilmenau, Germany, in 2017 and 2018, respectively. He is currently working at the Fraunhofer Institute for Integrated Circuits IIS. His research interests include passive radar technologies and high-resolution parameter estimation of radar signals.



Jian Luo received the B.A.Sc. degree in communication engineering from the South China University of Technology in 2004 and the M.S. and Ph.D. degrees in electrical engineering from Technische Universität Berlin, Germany, in 2006 and 2012, respectively. From 2007 to 2012, he was a researcher and project manager in the Fraunhofer Heinrich Hertz Institute in Berlin. Since October 2012, he is with Huawei

Technologies Duesseldorf GmbH, European Research Center, and works on 5G wireless communication systems. He has been involved/technical lead in a number of national-funded and EU-funded research projects, including

SAPHYRE, METIS, mmMAGIC, 5G-CAR, 5G-CROCO. His main research interests include millimeter wave communication technologies, air-interface design, channel modeling, positioning, RF impairment modeling and compensation.



Andreas Schwind received his B.Sc. and M.Sc. degrees in electrical engineering from Technische Universität Ilmenau in 2015 and 2017, respectively. As a researcher and doctoral student, he is currently working in the RF and Microwave Research Group at the Technische Universität Ilmenau. His research interests include bi-static radar measurements, and the analysis of radar signals in vehicular scenarios.



Reiner S. Thomä received his degrees in electrical engineering and information technology from Technische Universität Ilmenau, Germany. Since 1992, he has been a Professor of electrical engineering (electronic measurement technology) at the same University. With his group, he has contributed to several European and German research projects and clusters. His research interests include array signal processing, propagation measurement, and modeling, high-resolution parameter estimation, multidimensional channel sounding, over-the-air testing of multiple antenna systems in virtual electromagnetic environments, MIMO-, mmW-, and UWB-radar sensors for object detection and tracking, and joint communication and radar sensing (cooperative passive coherent location). In 2007, he was awarded IEEE Fellow and received the Thuringian State Research Award for Applied Research both for contributions to high-resolution multidimensional channel sounding. In 2014, he received the Vodafone Innovation Award.



Giovanni Del Galdo studied telecommunications engineering at Politecnico di Milano. In 2007, he received his doctoral degree from Technische Universität Ilmenau on the topic of MIMO channel modeling for mobile communications. He then joined Fraunhofer Institute for Integrated Circuits IIS working on audio watermarking and parametric representations of spatial sound. Since 2012, he leads a

joint research group composed of a department at Fraunhofer IIS and, as a full professor, a chair at TU Ilmenau on the research area of electronic measurements and signal processing. His current research interests include the analysis, modeling, and manipulation of multi-dimensional signals, over-the-air testing for terrestrial and satellite communication systems, and sparsity promoting reconstruction methods.